HHS Public Access

Author manuscript

Biol Psychiatry. Author manuscript; available in PMC 2021 June 01.

Published in final edited form as:

Biol Psychiatry. 2020 June 01; 87(11): 967–978. doi:10.1016/j.biopsych.2019.10.030.

Prefrontal regulation of punished ethanol self-administration

Lindsay R. Halladay[1,2,*], **Adrina Kocharian**[1], **Patrick T. Piantadosi**[1,5], **Michael E. Authement**[3,5], **Abby G. Lieberman**[1], **Nathen A. Spitz**[1], **Kendall Coden**[1], **Lucas R. Glover**[1], **Vincent D. Costa**[4], **Veronica A. Alvarez**[3,5], **Andrew Holmes**[1]

[1]Laboratory of Behavioral and Genomic Neuroscience, National Institute on Alcohol Abuse and Alcoholism, NIH, Bethesda, MD, USA

[2]Department of Psychology, Santa Clara University, Santa Clara, CA, USA

[3]Laboratory on Neurobiology of Compulsive Behaviors, National Institute on Alcohol Abuse and Alcoholism, NIH, Bethesda, MD, USA

[4]Department of Behavioral Neuroscience, Oregon Health Sciences University, Portland, OR, USA

[5]Center on Compulsive Behaviors, Intramural Research Program, NIH, Bethesda, USA

Abstract

Background: A clinical hallmark of alcohol use disorder (AUD) is persistent drinking despite potential adverse consequences. The ventral (vmPFC) and dorsal (dmPFC) medial prefrontal cortex are positioned to exert top-down control over subcortical regions, such as the nucleus accumbens shell (NAcS) and basolateral amygdala (BLA), which encode positive and negative valence of EtOH-related stimuli. Prior rodent studies have implicated these regions in regulation of punished EtOH self-administration (EtOH-SA).

Methods: We conducted *in vivo* electrophysiological recordings in mouse vmPFC and dmPFC to obtain neuronal correlates of footshock-punished EtOH-SA. *Ex vivo* recordings were performed in NAcS D1-positive MSNs receiving vmPFC input to examine punishment-related plasticity in this pathway. Optogenetic photosilencing was employed to assess the functional contribution of the vmPFC and dmPFC, vmPFC projections to NAcS or BLA, to punished EtOH-SA.

Results: Punishment reduced EtOH-lever pressing and elicited aborted presses (lever approach followed by rapid retraction). Neurons in vmPFC and dmPFC exhibited phasic firing to EtOH-lever presses and aborts, but only in vmPFC was there a population-level shift in coding from lever presses to aborts with punishment. Closed-loop vmPFC, not dmPFC, photosilencing on a post-punishment probe test negated the reduction in EtOH-lever presses but not aborts. Punishment was associated with altered plasticity at vmPFC inputs to D1-MSNs in NAcS. Photosilencing vmPFC

[*]Correspondence to: Lindsay R. Halladay PhD, Alumni Science Hall, Rm 204, Santa Clara University, 500 El Camino Real, Santa Clara, CA 95053, USA, telephone +14085513399, lhalladay@scu.edu.

Financial Disclosures

The authors report no biomedical financial interests or potential conflicts of interest.

projections to NAcS, not BLA, partially reversed suppression of EtOH-lever presses on probe testing.

Conclusions: These findings demonstrate a key role for vmPFC in regulating EtOH-SA after punishment, with implications for understanding the neural basis of compulsive drinking in AUDs.

Keywords

alcohol; compulsive; nucleus accumbens; amygdala; mouse; corticostriatal; infralimbic

Introduction

Excessive alcohol drinking is the third leading cause of preventable death in the United States (1). By recent estimates, over fifteen million adults are afflicted by alcohol use disorders (AUD), while a quarter of the adult population reports recently engaging in either heavy alcohol use or binge drinking (1). A hallmark of AUDs is that drinking persists despite an awareness of the potential adverse consequences (2). Despite a large body of work describing brain mechanisms underlying alcohol-seeking, the neural circuits that exert control over the drive to use alcohol and other drugs in the face of potential negative outcomes remain poorly understood (3–10).

There is growing evidence from human and rodent studies that the medial prefrontal cortex (mPFC) modulates ethanol self-administration (EtOH-SA), and has been shown to either reduce or enable various measures of EtOH-seeking and drinking (4, 5). For instance, cue-induced reinstatement of EtOH consumption is abolished by ablating neuronal ensembles in the ventromedial (vmPFC), but not dorsomedial (dmPFC) PFC (11, 12). The mPFC is also well-positioned, anatomically, to arbitrate between EtOH-seeking and avoidance via its connections with amygdaloid and striatal regions (13–17).

Prior studies have found that the development of resistance to EtOH-SA is associated with plasticity in mPFC projections to the NAc core (NAcC) (18), and that disconnecting dmPFC from NAcC biases rats towards making disadvantageous decisions (19, 20). Moreover, recent data has shown that the shell region of NAc (NAcS) and basolateral amygdala (BLA), as well as mPFC connections with these regions, play a key role in regulating responding to non-drug rewards in the presence of reward-associated cues and potentially aversive outcomes (21–27). These circuits are also affected by EtOH exposure. For example, EtOH dependence was accompanied by insertion of GluA2-lacking AMPA-receptors at glutamatergic synapses in NAc MSNs (28) and increased excitability and amplitude of NMDA receptor-mediated synaptic responses in D1-expressing NAc MSNs (29). Furthermore, NMDA receptors in the NAc and medial prefrontal cortex (mPFC) are implicated in punishment-resistant EtOH-drinking in rats (18, 30), and a recent elegant study found activity of NAc-projecting vmPFC neurons predicted lesser cocaine-seeking (27).

Taken together, these prior studies suggest that vmPFC, BLA, and NAc are part of an integrated circuit regulating the seeking, consumption and, in the face of negative outcomes, avoidance of EtOH and other drugs of abuse (31–36). Nonetheless, understanding of the contributions of the vmPFC and its downstream connections to BLA and NAcS to the

regulation of punished EtOH-SA remains incomplete. The aim of the current study was to clarify this role using a combination of *in vivo* and *ex vivo* neuronal recordings and optogenetic manipulations in a mouse assay for punished EtOH-SA.

Methods and Materials

Subjects

Subjects were male (7-8 weeks old) C57BL/6J and B6.Cg-Tg(Drd1a-tdTomato)6Calak/J mice obtained from The Jackson Laboratory, gradually reduced to 85% of their free-feeding body weight before testing.

Ethical considerations

All experimental procedures were approved by the NIAAA Animal Care and Use Committee and followed the NIH guidelines outlined in Using Animals in Intramural Research.

Behavioral testing

Mice were trained in a Med Associates operant chamber to respond on the left of 2 levers on a continuous schedule of reinforcement to earn sucrose pellets during 40-min sessions (right, 'inactive-lever' had no programed consequences) until criterion was met (>35 rewards) as previously described (37–39). The pellet was then substituted with a progression of 10μL liquid-rewards ("sucrose fading"; 10% sucrose, 10% sucrose+10% EtOH, 5% sucrose+10% EtOH, 10% EtOH). Training at each EtOH-concentration stage continued until performance was stable (<20% coefficient between reward-lever responses over 3 sessions).

There was then a single punishment session consisting of a baseline-period (10 rewarded/unpunished EtOH-lever presses) immediately followed (after the 10^{th} press) by a 40-min punishment period (EtOH-lever presses alternatingly produced 10% EtOH or no-EtOH +footshock). A probe test (identical to rewarded training sessions) was conducted 24hr later. For *in vivo* recordings, a second probe was conducted 24-hr following the first, with data collapsed across probes for analyses. EtOH-lever presses, inactive-presses, and head-entries into the reward receptacle were recorded by Med-PC software. Approaches to the EtOH-lever with an elongated body posture, followed by rapid body-retraction without execution of press were scored manually (Supplemental Video 1) and referred to as 'aborts,' keeping with the definition of a similar behavior in rats (40).

In vivo neuronal recordings

Following training, fixed microelectrode arrays, were surgically implanted in bilateral vmPFC and dmPFC of the same mouse (41, 42). Recordings were conducted during punishment and probe testing using OmniPlex Neural Data Acquisition System combined with simultaneous CinePlex Behavioral Research Systems (41). Mean firing rate of recorded cells was 6.33±0.90 for vmPFC and 4.12±0.46 for dmPFC.

Spike timestamp information was integrated and analyzed using NeuroExplorer. For each unit, spikes were time-locked to the onset of behavioral events. Spiking activity 1s prior to

event onset was used as baseline. Using a sliding window (300ms) stepped in 10ms bins from −2.5s to +2.5s around each event, we computed *t*-tests to determine when the activity surrounding each event deviated from baseline; units with significant deviations were considered responsive to an event for that time bin.

Fluorescence in situ hybridization (FISH)

Immediately after probe testing, brains were collected to perform FISH using the RNAscope Multiplex Fluorescent Assay Kit (42) to label vmPFC *fos* (c-fos), *Slc17a7* (vGluT1), *Gad1* (Gad67), *Drd1a* (DR1A), and *Drd2* (DR2). We used ImageJ to calculate percentage of DAPI-labeled neurons positive for *fos,* and of those, the percentage that were *Slc17a7−, Gad1−, Drd1a−,* and *Drd2*-positive.

Ex vivo whole-cell recordings

AAV5/CaMKIIα-hChR2(H134R)-eYFP was bilaterally injected into the vmPFC of D1-tdTomato mice. Mice underwent behavioral testing and were scarified on probe day. Cells in NAcS brain sections were voltage-clamped at +40mV (in gabazine). tdTomato-expressing D1-MSNs and non-fluorescent putative D2-MSNs were identified using blue light-pulses to optically evoke EPSCs. AMPA-mediated EPSCs were pharmacologically isolated using (R)-CPP, and subtracted from combined EPSCs to obtain the NMDA-mediated EPSC component (28). AMPA:NMDA ratios were calculated by dividing peak receptor-mediated EPSC by peak NMDA-mediated EPSC. For rectification index, AMPA-mediated EPSCs were measured at both negative and positive (−55/+40 mV) holding potentials and spermine was included in the internal solution. Rectification index was calculated by dividing peak current at −55mV by peak current at +40 mV.

In vivo photosilencing

rAAV8/CAG-ArchT-GFP or rAAV8/CAG-GFP (local PFC-silencing) or AAV5/CaMKIIα-eArchT3.0-eYFP or AAV5/CaMKII-eYFP (vmPFC projection-silencing) was bilaterally injected into vmPFC or dmPFC, and optic fiber-containing ferrules were implanted either locally or in terminal regions (NAcS/BLA) (43, 44). One month later, mice underwent reminder-training sessions, then punishment and probe testing. During the probe test, green light was shone when the mouse was in a zone (~2.75x4 inches) around the EtOH-lever, determined in real-time by CinePlex software.

Retrograde neuronal tracing

Retrograde tracers Cholera Toxin B (CTb555/488) were injected into NAcS and BLA of the same mouse. Seven days later, brain mPFC sections were inspected for cell bodies labeled with either or both fluorophore (45).

Statistical analysis

Data were analyzed using Student's t-tests, ANOVA followed by Newman-Keuls and Šidák corrected *post hoc* tests, and bivariate correlation.

Results

Punishment suppresses EtOH-SA

We first examined the behavioral profile of mice undergoing *in vivo* neuronal recordings. Replicating previous observations (37–39), the rate of EtOH-lever pressing was significantly suppressed during punishment and probe testing, compared to the unpunished baseline period of the punishment session (Figure 1B–C). The number of shocks received inversely predicted suppression on probe (i.e., positive correlation between EtOH-SA during punishment and probe; r=.61, P=.003), showing that the degree of suppression during probe testing was not due to the number of shocks received. Head-entries were also significantly reduced following punishment (Figure S2), whereas inactive-lever presses increased slightly during punishment, but returned to low levels on probe. Another important observation was the emergence of EtOH-lever press aborts during punishment and maintained on the probe tests (Figure 1B–C). This behavior reflects the development of a conflict between EtOH-seeking and shock-avoidance, and has been described in rat punishment paradigms (40).

Neuronal correlates of punished EtOH-SA

We next tested for *in vivo* neuronal correlates of behavior by recording the activity of 191 vmPFC and 195 dmPFC neurons in 20 mice (Figure 2A). In both brain regions, we detected examples of individual neurons exhibiting increases or decreases in firing around the time mice made either an EtOH-lever press or an abort (Figure 2B–C). We did not classify these behavior-related cells as putative glutamatergic projection neurons verses interneurons based on spiking characteristics. However, FISH-labeling of *fos* and mRNA markers for glutamatergic and GABAergic phenotypes (Figure 2D–E), showed that of those cells by probe testing, the vast majority were glutamatergic (Figure 2F). This echoes data from other EtOH-SA tasks (e.g., reinstatement) showing that most activated cells are glutamatergic (11).

vmPFC-coding punished of EtOH-SA

We next examined population-level mPFC-coding (46) by aligning neuronal firing in a 5-sec window around behavioral events during the pre-punishment baseline, punishment, and probe tests. During baseline, we found clear population-level representation of EtOH-lever presses in vmPFC (~30% of units, n=65); neuronal engagement increased over the 1.5sec prior to execution of a lever-press and peaked slightly after a press was made (Figure 2G). During the punished phase, press-related activity of vmPFC neurons was minimal (Figure 2H) but there was strong coding of aborts (~38% of vmPFC units) beginning around 0.5sec prior to the mouse retracting away from the EtOH-lever (Figure 2I). Notably, this vmPFC neuronal coding of aborts was maintained during probe testing, while coding of EtOH-lever presses returned to levels evident during punishment, despite the fact that the number of presses was still much lower (Figure 2J–K). To determine whether EtOH-lever and abort events were encoded by distinct neural populations in vmPFC, we conducted a correlational analysis on units that were responsive to either event. Interestingly, only 2 of all units recorded exhibited firing rates during the two events that correlated significantly, suggesting that these behaviors are represented by separate ensembles in vmPFC.

These *in vivo* neuronal data demonstrate that vmPFC neurons exhibit representations of the execution of a response for EtOH and avoidance of that same response in a manner that shifts depending on the prevailing task demands: pre-punishment=press, ongoing punishment=abort. This agrees with previous studies showing the vmPFC can contribute to the promotion or inhibition of reward-seeking across different experimental situations (31, 34, 47–53). The current data also show that during probe testing, when there is prior knowledge of both the reward and punishment outcomes for responding, the vmPFC strongly codes for both lever-pressing and aborts, consistent with a role in arbitrating between opposing actions under conflict, but not a simple response-suppression function.

Silencing vmPFC abolishes punished-suppression of EtOH-SA

Our recording data demonstrate vmPFC neuronal correlates of punished-suppression of EtOH-SA, but do not address causal contribution of vmPFC to performance. Therefore, we devised a 'closed-loop' optogenetic approach to test the consequences of photosilencing ArchT-transfected vmPFC neurons when mice were near the EtOH-lever during the probe test (Figure 3A–C).

We found that silencing vmPFC neurons in this manner abolished punishment-induced suppression of EtOH-SA. Specifically, GFP-expressing control mice exhibited a significant decrease in EtOH-lever pressing during probe testing, relative to the last training day prior to punishment, whereas there was no significant change in ArchT animals such that their probe test lever-pressing was significantly higher than GFP mice (Figure 3D). Notably, despite this silencing-induced normalization of lever-pressing, aborts exhibited by the groups did not differ (Figure 3E), nor did the cumulative or average time spent in the light-on zone proximal to the EtOH-lever (Figure 3F), or inactive-lever presses (Figure 3G). There was a small but significant increase in head-entries in ArchT mice but not GFP controls (Figure 3H), which likely reflects more frequent reward-collection/checking in the higher-pressing ArchT group, rather than greater motivation for the EtOH-reward following vmPFC-silencing. Indeed prior studies in rats report negative (54, 55) or *de*motivating (56–59) effects on reward-seeking after vmPFC lesioning and pharmacological inactivation.

In a control experiment, mice underwent the same behavioral testing and surgical procedures, then on reaching training criterion, were given a pseudo-probe test (i.e., without punishment) during which the vmPFC was silenced (exactly as above). All behavioral parameters were similar between ArchT and GFP groups (Figure S13), demonstrating that vmPFC-silencing was insufficient to alter behavior in the absence of punishment, excluding the possibility that increased EtOH-SA in punished mice following vmPFC-silencing was due to a general increase in motivation for EtOH-SA.

dmPFC-coding of punished EtOH-SA

We next determined whether the contribution of the vmPFC to punished EtOH-SA was shared by neighboring dmPFC. Recorded units in the dmPFC did not show the same shifts in task-phase related population-coding seen in vmPFC, though there was moderate dmPFC activity associated with EtOH-lever and abort events during probe testing (Figure 4A–E). Prior work has suggested that dmPFC promotes reward-SA (31), a notion supported by

recent reports of *in vivo* calcium transients evident during sucrose-cue presentation in dmPFC and dmPFC→NAcC cells (60). Indeed, data here indicate an absence of clear neuronal correlates in dmPFC during punishment, but it remains possible that representations are extant but restricted to discrete dmPFC ensembles that are difficult to resolve with neuronal recordings. Related, a recent report found a small subset of shock-activated NAcS-projecting dmPFC cells exhibited calcium correlates during avoidance of punished-reward (22).

dmPFC-photosilencing does not affect punished-suppression of EtOH-SA

We next assessed the consequences of photosilencing the dmPFC, employing the same closed-loop design described above (Figure 4F), anticipating that the lack of EtOH-SA correlates in dmPFC would correspond with minimal functional relevance. In contrast to vmPFC effects, following dmPFC-silencing, EtOH-lever press rates in ArchT and GFP groups were similarly decreased following punishment (Figure 4G). Likewise, aborts, time spent in the light-on EtOH-lever zone, inactive-lever presses, and head-entries were all unaffected by dmPFC-silencing (Figure 4H–K).

These optogenetic data show that, in contrast to the vmPFC, dmPFC is not necessary for the expression of punished-suppression.

Punished-suppression of EtOH-SA produces vmPFC→NAc plasticity

Our next step was to identify vmPFC outputs that modulate punished-suppression, focusing on the NAcS. We tested for plastic changes to synaptic inputs selectively from vmPFC to NAcS associated with punished EtOH-SA, focusing on D1-expressing MSNs given the cell-specificity of EtOH-induced changes described in the introduction and the report that pharmacologically blocking D1-receptors in NAcS promotes EtOH-(and sucrose) SA elicited by conditioned cues/contexts (25, 62–66). Indeed, FISH-labeling of *fos* and mRNA markers for D1- and D2-expressing neuronal phenotypes, showed that the large majority of probe testing-activated (*fos*-positive) NAcS MSNs were D1-expressing (Figure S5).

After probe testing, glutamatergic synaptic responses (EPSCs) were evoked in D1-expressing MSNs (red cells, D1-tdTomato reporter) and for comparison, putative D2-expressing MSNs (non-red cells) in NAcS by ChR2-mediated light-stimulation of vmPFC inputs (Figure 5A, S7). These recordings revealed a significant decrease in AMPA:NMDA ratio at glutamatergic inputs to D1-expressing MSNs in the punished group, compared to unpunished controls (Figure 5B, S7), but no significant difference in AMPA:NMDA ratio at glutamatergic inputs to putative D2-expressing MSNs (Figure S7). This suggests preferential synaptic plasticity at vmPFC inputs to NAcS D1-MSNs following punishment and probe testing. Of further note, punishment did not change the rectification index, (i.e., contribution of GluA2 subunit to the AMPA response), in D1R or D2R-expressing MSNs (Figure 5C–D, S7), indicating that AMPA:NMDA ratio reductions were not associated with any obvious change in AMPA receptor subunit composition.

These *ex vivo* recording data show evidence of plasticity at vmPFC→D1 MSNs inputs in the NAcS as a consequence of punishment.

Silencing vmPFC→NAcS, not vmPFC→BLA, attenuates punished-suppression of EtOH-SA

We next asked whether the punishment-related plastic changes in the vmPFC→NAcS reflect a causal contribution of this pathway. Employing the same closed-loop photosilencing procedure used for local PFC-silencing, we shone green light into the NAcS to inhibit ArchT-transfected fibers originating from vmPFC during probe testing (Figure 5E). YFP controls showed a significant decrease in EtOH-lever pressing, but the corresponding decrease in ArchT animals was comparably smaller and non-significant, such that YFP and ArchT groups differed significantly (Figure 5F). The rate of aborts, inactive-lever presses, and time spent in the EtOH-lever zone did not differ between groups, but head-entry rate was slightly higher in the ArchT group, in line with their slightly higher rate of EtOH-lever pressing (Figure 5G–H, S9).

We compared the behavioral effects of vmPFC→NAcS-silencing with those of a parallel pathway, vmPFC→BLA (Figure 5I). Silencing vmPFC→BLA projections did not affect any measure for YFP or ArchT groups (Figure 5J–L, S11).

These data extend our recording and optogenetic data implicating the vmPFC in punished-suppression of EtOH-SA by showing that vmPFC interacts with NAcS to some extent to modulate this behavior.

Minimal collateralization of vmPFC neurons to NAcS and BA

While optogenetics experiments were designed to selectively target vmPFC→NAcS/BLA, it is possible that non-selective effects occurred through inhibition of vmPFC neurons sending collaterals to both regions. To address this, Alexa-conjugated CTb (555/488) were injected into NAcS and BLA to retrogradely-label neurons in mPFC. Consistent with recent, methodologically similar work quantifying vmPFC collateralization to NAcS and BLA (45), we saw very few double-labeled cells in vmPFC or dmPFC (Figure S12), suggesting the attenuated punished-suppression effect of vmPFC→NAcS-silencing is unlikely to stem from effects on vmPFC→NAcS/BLA collaterals, though we cannot exclude the contribution of vmPFC collaterals to other brain regions.

Discussion

Collectively, these data provide correlative and causal evidence supporting an important contribution of the vmPFC in regulating EtOH-SA in the face of potential punishment.

Two key findings in the current study were that 1) following punishment, vmPFC neurons coded EtOH-lever pressing and were behaviorally required for the suppression of lever-pressing, and 2) while vmPFC neurons also strongly coded for aborting EtOH-lever pressing after punishment, vmPFC was not necessary for expression of this avoidance beahvior. These data fit with the long-standing view of the importance of this region for inhibitory control over various processes at play in the current task, most pertinently reward-seeking and threat-avoidance (61, 62).

As noted, a striking observation was that despite clear evidence for neural representation of abort-behavior within vmPFC, optogenetically silencing vmPFC did not reduce the number

of aborts made during probe testing. This dichotomy suggests that despite the disinhibited EtOH-seeking induced by vmPFC-silencing, the association between the EtOH-lever response and the punished outcome was retained and expressed. A related conclusion is that brain regions other than vmPFC (e.g., periaqueductal gray or certain amygdaloid nuclei) either normally mediate abort expression, or can maintain abort-behavior when the vmPFC is non-functional. These data support a model in which rather than being a simple substrate for inhibiting EtOH-SA, the role of vmPFC is more complex in signaling changes in response-outcome relationships after punishment, which, in turn, enables appropriate modification of some (lever-pressing) but not all (aborts) behaviors.

It is becoming increasingly clear that the vmPFC and dmPFC can contribute to reward-related behaviors in complementary or contrasting ways, depending on factors not limited to the testing context and history with or type of drug/reward (53). Further speaking to this complexity, we found that, in contrast to vmPFC-silencing, silencing the dmPFC using the same experimental design was without effect. On the one hand, these negative findings concur with recent work showing that pharmacologically inactivating rat dmPFC did not affect punished EtOH-lever pressing (55) or conditioned avoidance-behavior (63). On the other hand, a lack of dmPFC-silencing effects is perhaps surprising in view of the neural correlates of probe performance we detected in dmPFC, as well as earlier data from rats showing that dmPFC-inactivation or photosilencing increased punished licking for water (64) and promoted punished cocaine-seeking (65, 66).

There may be technical reasons for these discrepancies, such as species idiosyncrasies or differences in drug or behavioral assays used. A more interesting possibility, however, is that dmPFC does indeed contribute to punished EtOH-SA, but this effect is difficult to uncover due to functional heterogeneity across dmPFC neurons: our neuronal recordings indicated the presence of both inhibitory and excitatory coding of presses and aborts in dmPFC during probe testing. In this regard, a recent study found that photoexcitation of dmPFC→NAcS only reduced punished responding for a milkshake reward (albeit partially) when shock-activated dmPFC neurons were selectively manipulated (22). Thus, similarly targeted manipulations of task-related neuronal ensembles may be required to unmask a role for the dmPFC in punished EtOH-SA.

Providing initial insight into downstream targets of the vmPFC that are recruited to regulate punished EtOH-SA, we found evidence of plasticity of vmPFC inputs to NAcS D1-MSNs suggestive of a punishment-induced change in synaptic strength of these inputs. This plasticity appeared restricted to input onto D1-MSNs, but not putative D2-MSNs. Incubation of cocaine-seeking has been associated with strengthening of vmPFC inputs onto NAcS D1-MSNs, as evidenced by the formation of silent synapses, which when optogenetically reversed, produces either increased or decreased cocaine-responding (67, 68).

If the vmPFC reduced EtOH-lever pressing after punishment via downstream connections to NAcS, the most parsimonious prediction would be behavioral suppression associated with strengthening of vmPFC inputs to NAcS D1-MSNs. Our finding of reduced D1-MSN AMPA:NMDA ratios, however, appears more in-line with a depotentiation in this pathway. One possible explanation is that this change is indicative of a postsynaptic homeostatic

change in NAcS MSNs that could relate to the recruitment of the vmPFC and increased drive onto these cells with punishment. Equally plausible is the interpretation that the changes result from altered inputs from other regions, or in microcircuits within the NAcS itself. Further work will be needed to parse these possibilities.

Prior work has shown that ablating mPFC→NAcS neurons reduces EtOH-reinstatement (17), while activating vmPFC→NAc reduces cocaine-seeking (27), and disconnecting the vmPFC→NAcS pathway produces heroin-relapse (69). We found that silencing the vmPFC→NAcS pathway attenuated a punishment-induced decrease in EtOH-lever pressing. Of note, this effect was characterized by a partial reversal of suppression, rather the full reversal seen with local vmPFC-silencing. This difference could be explained in various ways. One reason could be the use of a CaMKII-promoter to express ArchT in vmPFC. This promoter prefers, but is not exclusive to, glutamatergic neurons, leaving open the possible contribution of silencing long-range GABAergic interneurons, which could have different or opposite effects to those produced by glutamatergic projection-silencing (70). Another explanation is that vmPFC→NAcS silencing does not fully recapitulate the effects of local vmPFC-silencing because of the contribution of other efferent projections of vmPFC. Although the identity of these is unclear, our negative optogenetic data indicate that vmPFC→BLA does not critically mediate punished-suppression in the current task, despite evidence supporting a role for the BLA in other assays of punished reward-seeking (23, 71).

A third, particularly intriguing possibility again raises the issue of functional heterogeneity at the level of the NAcS itself. If distinct subpopulations of NAcS cells promote EtOH-SA, while others mediate suppression, it would not be surprising that the net effect of non-discriminately silencing vmPFC inputs to NAcS would be mixed. In this context, vmPFC-inactivation has been found to disinhibit a subpopulation of NAcS neurons encoding reward-seeking suppression, while simultaneously inhibit another population of reward-encoding NAcS cells (72). Recent work also shows that with VTA-DA inputs to NAcS, effects on reward-seeking and aversion can be opposite, depending on the sub-compartment and cell-type targeted (26, 73). Finally, in terms of their outputs, NAcS cells targeting the VTA versus lateral hypothalamus have opposite effects on context-induced EtOH-relapse (74). Thus, the vmPFC→NAcS circuit is positioned to exert inhibitory and excitatory influences on consumption and responding for rewards including EtOH (75–78). An important future question will be defining the contribution of inputs from vmPFC,(as well as BLA) (17, 79, 80) to specific functional classes of NAcS neurons involved in punished-suppression of EtOH-SA.

Functional perturbation of the PFC has been consistently reported in AUDs and in animal models of EtOH-exposure, which can lead to a shift towards less-flexible behaviors mediated by subcortical structures (81–83). These shifts are thought to contribute to the progression from moderate drinking to uncontrolled, compulsive alcohol abuse. Consistent with this, the current study shows that the vmPFC codes for behaviors associated with the avoidance of a punished response for EtOH and is required for the suppression of EtOH-SA after punishment. Further, the current results show that vmPFC interacts with the NAcS to modulate punished EtOH-SA behavior. Collectively, these findings advance our understanding of the neural circuits that may underlie compulsive drinking.

Supplementary Material

Refer to Web version on PubMed Central for supplementary material.

Acknowledgements

Work supported by the NIAAA Intramural Research Program (ZIA-AA000401) to AH and the Intramural Programs of NIAAA and NINDS (ZIA-AA000421) to VAA, Postdoctoral Research Associate Training fellowship from the Center on Compulsive Behaviors to PTP and MEA, and NIH Director's Challenge Award and DDIR Innovation Award to VAA.

References

1. Substance Abuse and Mental Health Services Administration S (2015): National Survey on Drug Use and Health (NSDUH). https://wwwsamhsagov/data/sites/default/files/NSDUH-DetTabs-2015/NSDUH-DetTabs-2015/NSDUH-DetTabs-2015htm#tab2-46b.
2. DSM-5 (2013): Diagnostic and Statistical Manual of Mental Disorders. Fourth Edition ed. Washington, D.C.: APA Press.
3. Tuesta LM, Chen Z, Duncan A, Fowler CD, Ishikawa M, Lee BR, et al. (2017): GLP-1 acts on habenular avoidance circuits to control nicotine intake. Nature neuroscience. 20:708–716. [PubMed: 28368384]
4. Everitt BJ, Robbins TW (2005): Neural systems of reinforcement for drug addiction: from actions to habits to compulsion. Nature neuroscience. 8:1481–1489. [PubMed: 16251991]
5. Koob GF, Volkow ND (2010): Neurocircuitry of addiction. Neuropsychopharmacology : official publication of the American College of Neuropsychopharmacology. 35:217–238. [PubMed: 19710631]
6. Hopf FW, Lesscher HM (2014): Rodent models for compulsive alcohol intake. Alcohol. 48:253–264. [PubMed: 24731992]
7. Jean-Richard-Dit-Bressel P, Killcross S, McNally GP (2018): Behavioral and neurobiological mechanisms of punishment: implications for psychiatric disorders. Neuropsychopharmacology : official publication of the American College of Neuropsychopharmacology.
8. Orsini CA, Moorman DE, Young JW, Setlow B, Floresco SB (2015): Neural mechanisms regulating different forms of risk-related decision-making: Insights from animal models. Neuroscience and biobehavioral reviews. 58:147–167. [PubMed: 26072028]
9. Marchant NJ, Campbell EJ, Pelloux Y, Bossert JM, Shaham Y (2018): Context-induced relapse after extinction versus punishment: similarities and differences. Psychopharmacology.
10. Giuliano C, Pena-Oliver Y, Goodlett CR, Cardinal RN, Robbins TW, Bullmore ET, et al. (2018): Evidence for a Long-Lasting Compulsive Alcohol Seeking Phenotype in Rats. Neuropsychopharmacology : official publication of the American College of Neuropsychopharmacology. 43:728–738. [PubMed: 28553834]
11. Pfarr S, Meinhardt MW, Klee ML, Hansson AC, Vengeliene V, Schonig K, et al. (2015): Losing Control: Excessive Alcohol Seeking after Selective Inactivation of Cue-Responsive Neurons in the Infralimbic Cortex. The Journal of neuroscience : the official journal of the Society for Neuroscience. 35:10750–10761. [PubMed: 26224858]
12. Meinhardt MW, Hansson AC, Perreau-Lenz S, Bauder-Wenz C, Stahlin O, Heilig M, et al. (2013): Rescue of Infralimbic mGluR2 Deficit Restores Control Over Drug-Seeking Behavior in Alcohol Dependence. The Journal of neuroscience : the official journal of the Society for Neuroscience. 33:2794–2806. [PubMed: 23407939]
13. Groenewegen HJ, Wright CI, Beijer AV, Voorn P (1999): Convergence and segregation of ventral striatal inputs and outputs. Annals of the New York Academy of Sciences. 877:49–63. [PubMed: 10415642]
14. Sesack SR, Deutch AY, Roth RH, Bunney BS (1989): Topographical organization of the efferent projections of the medial prefrontal cortex in the rat: an anterograde tract-tracing study with Phaseolus vulgaris leucoagglutinin. J Comp Neurol. 290:213–242. [PubMed: 2592611]

15. Krettek JE, Price JL (1977): Projections from the amygdaloid complex to the cerebral cortex and thalamus in the rat and cat. J Comp Neurol. 172:687–722. [PubMed: 838895]
16. Brog JS, Salyapongse A, Deutch AY, Zahm DS (1993): The patterns of afferent innervation of the core and shell in the “accumbens” part of the rat ventral striatum: immunohistochemical detection of retrogradely transported fluoro-gold. J Comp Neurol. 338:255–278. [PubMed: 8308171]
17. Keistler CR, Hammarlund E, Barker JM, Bond CW, DiLeone RJ, Pittenger C, et al. (2017): Regulation of Alcohol Extinction and Cue-Induced Reinstatement by Specific Projections among Medial Prefrontal Cortex, Nucleus Accumbens, and Basolateral Amygdala. The Journal of neuroscience : the official journal of the Society for Neuroscience. 37:4462–4471. [PubMed: 28336571]
18. Seif T, Chang SJ, Simms JA, Gibb SL, Dadgar J, Chen BT, et al. (2013): Cortical activation of accumbens hyperpolarization-active NMDARs mediates aversion-resistant alcohol intake. Nature neuroscience. 16:1094–1100. [PubMed: 23817545]
19. St Onge JR, Stopper CM, Zahm DS, Floresco SB (2012): Separate prefrontal-subcortical circuits mediate different components of risk-based decision making. The Journal of neuroscience : the official journal of the Society for Neuroscience. 32:2886–2899. [PubMed: 22357871]
20. St Onge JR, Floresco SB (2010): Prefrontal cortical contribution to risk-based decision making. Cerebral cortex. 20:1816–1828. [PubMed: 19892787]
21. Burgos-Robles A, Kimchi EY, Izadmehr EM, Porzenheim MJ, Ramos-Guasp WA, Nieh EH, et al. (2017): Amygdala inputs to prefrontal cortex guide behavior amid conflicting cues of reward and punishment. Nature neuroscience. 20:824–835. [PubMed: 28436980]
22. Kim CK, Ye L, Jennings JH, Pichamoorthy N, Tang DD, Yoo AW, et al. (2017): Molecular and Circuit-Dynamical Identification of Top-Down Neural Mechanisms for Restraint of Reward Seeking. Cell. 170:1013–1027 e1014. [PubMed: 28823561]
23. Piantadosi PT, Yeates DCM, Wilkins M, Floresco SB (2017): Contributions of basolateral amygdala and nucleus accumbens subregions to mediating motivational conflict during punished reward-seeking. Neurobiology of learning and memory. 140:92–105. [PubMed: 28242266]
24. Piantadosi PT, Yeates DCM, Floresco SB (2018): Cooperative and dissociable involvement of the nucleus accumbens core and shell in the promotion and inhibition of actions during active and inhibitory avoidance. Neuropharmacology. 138:57–71. [PubMed: 29800544]
25. Keistler C, Barker JM, Taylor JR (2015): Infralimbic prefrontal cortex interacts with nucleus accumbens shell to unmask expression of outcome-selective Pavlovian-to-instrumental transfer. Learning & memory. 22:509–513. [PubMed: 26373829]
26. de Jong JW, Afjei SA, Pollak Dorocic I, Peck JR, Liu C, Kim CK, et al. (2019): A Neural Circuit Mechanism for Encoding Aversive Stimuli in the Mesolimbic Dopamine System. Neuron. 101:133–151 e137. [PubMed: 30503173]
27. Cameron CM, Murugan M, Choi JY, Engel EA, Witten IB (2019): Increased Cocaine Motivation Is Associated with Degraded Spatial and Temporal Representations in IL-NAc Neurons. Neuron. 103:80–91 e87. [PubMed: 31101395]
28. Laguesse S, Morisot N, Shin JH, Liu F, Adrover MF, Sakhai SA, et al. (2017): Prosapip1-Dependent Synaptic Adaptations in the Nucleus Accumbens Drive Alcohol Intake, Seeking, and Reward. Neuron. 96:145–159 e148. [PubMed: 28890345]
29. Renteria R, Maier EY, Buske TR, Morrisett RA (2017): Selective alterations of NMDAR function and plasticity in D1 and D2 medium spiny neurons in the nucleus accumbens shell following chronic intermittent ethanol exposure. Neuropharmacology. 112:164–171. [PubMed: 26946430]
30. LaLumiere RT, Smith KC, Kalivas PW (2012): Neural circuit competition in cocaine-seeking: roles of the infralimbic cortex and nucleus accumbens shell. The European journal of neuroscience. 35:614–622. [PubMed: 22321070]
31. Peters J, Kalivas PW, Quirk GJ (2009): Extinction circuits for fear and addiction overlap in prefrontal cortex. Learning & memory. 16:279–288. [PubMed: 19380710]
32. Floresco SB (2015): The nucleus accumbens: an interface between cognition, emotion, and action. Annu Rev Psychol. 66:25–52. [PubMed: 25251489]
33. Gourley SL, Taylor JR (2016): Going and stopping: Dichotomies in behavioral control by the prefrontal cortex. Nature neuroscience. 19:656–664. [PubMed: 29162973]

34. Peters J, LaLumiere RT, Kalivas PW (2008): Infralimbic prefrontal cortex is responsible for inhibiting cocaine seeking in extinguished rats. The Journal of neuroscience : the official journal of the Society for Neuroscience. 28:6046–6053. [PubMed: 18524910]
35. Orsini CA, Heshmati SC, Garman TS, Wall SC, Bizon JL, Setlow B (2018): Contributions of medial prefrontal cortex to decision making involving risk of punishment. Neuropharmacology. 139:205–216. [PubMed: 30009836]
36. Hopf FW, Bowers MS, Chang SJ, Chen BT, Martin M, Seif T, et al. (2011): Reduced nucleus accumbens SK channel activity enhances alcohol seeking during abstinence. Neuron. 65:682–694.
37. Radke AK, Jury NJ, Kocharian A, Marcinkiewcz CA, Lowery-Gionta EG, Pleil KE, et al. (2017): Chronic EtOH effects on putative measures of compulsive behavior in mice. Addiction biology. 22:423–434. [PubMed: 26687341]
38. Halladay LR, Kocharian A, Holmes A (2017): Mouse strain differences in punished ethanol self-administration. Alcohol. 58:83–92. [PubMed: 27814928]
39. Jury NJ, Pollack GA, Ward MJ, Bezek JL, Ng AJ, Pinard CR, et al. (2017): Chronic Ethanol During Adolescence Impacts Corticolimbic Dendritic Spines and Behavior. Alcoholism, clinical and experimental research. 41:1298–1308.
40. Hunt HF, Brady JV (1955): Some effects of punishment and intercurrent anxiety on a simple operant. J Comp Physiol Psychol. 48:305–310. [PubMed: 13252162]
41. Gamble-George JC, Baldi R, Halladay L, Kocharian A, Hartley N, Silva CG, et al. (2016): Cyclooxygenase-2 inhibition reduces stress-induced affective pathology. eLife. 5.
42. Gunduz-Cinar O, Brockway E, Lederle L, Wilcox T, Halladay LR, Ding Y, et al. (2018): Identification of a novel gene regulating amygdala-mediated fear extinction. Molecular psychiatry.
43. Bukalo O, Pinard C, Silverstein S, Brehm C, Hartley N, Whittle N, et al. (2015): Prefrontal inputs to the amygdala instruct fear extinction memory formation. Science Advances. 1:e1500251. [PubMed: 26504902]
44. Bergstrom HC, Lipkin AM, Lieberman AG, Pinard CR, Gunduz-Cinar O, Brockway ET, et al. (2018): Dorsolateral Striatum Engagement Interferes with Early Discrimination Learning. Cell reports. 23:2264–2272. [PubMed: 29791838]
45. Bloodgood DW, Sugam JA, Holmes A, Kash TL (2018): Fear extinction requires infralimbic cortex projections to the basolateral amygdala. Translational psychiatry. 8:60. [PubMed: 29507292]
46. Seo M, Lee E, Averbeck BB (2012): Action selection and action value in frontal-striatal circuits. Neuron. 74:947–960. [PubMed: 22681697]
47. Marchant NJ, Furlong TM, McNally GP (2010): Medial dorsal hypothalamus mediates the inhibition of reward seeking after extinction. The Journal of neuroscience : the official journal of the Society for Neuroscience. 30:14102–14115. [PubMed: 20962231]
48. Rhodes SE, Killcross S (2004): Lesions of rat infralimbic cortex enhance recovery and reinstatement of an appetitive Pavlovian response. Learning & memory. 11:611–616. [PubMed: 15466316]
49. Peters J, Vallone J, Laurendi K, Kalivas PW (2008): Opposing roles for the ventral prefrontal cortex and the basolateral amygdala on the spontaneous recovery of cocaine-seeking in rats. Psychopharmacology. 197:319–326. [PubMed: 18066533]
50. Barker JM, Torregrossa MM, Taylor JR (2012): Low prefrontal PSA-NCAM confers risk for alcoholism-related behavior. Nature neuroscience. 15:1356–1358. [PubMed: 22922785]
51. Ferenczi EA, Zalocusky KA, Liston C, Grosenick L, Warden MR, Amatya D, et al. (2016): Prefrontal cortical regulation of brainwide circuit dynamics and reward-related behavior. Science. 351:aac9698. [PubMed: 26722001]
52. Barker JM, Glen WB, Linsenbardt DN, Lapish CC, Chandler LJ (2017): Habitual Behavior Is Mediated by a Shift in Response-Outcome Encoding by Infralimbic Cortex. eNeuro. 4.
53. Moorman DE, James MH, McGlinchey EM, Aston-Jones G (2015): Differential roles of medial prefrontal subregions in the regulation of drug seeking. Brain research. 1628:130–146. [PubMed: 25529632]
54. Pelloux Y, Murray JE, Everitt BJ (2013): Differential roles of the prefrontal cortical subregions and basolateral amygdala in compulsive cocaine seeking and relapse after voluntary abstinence in rats. The European journal of neuroscience.

55. Jean-Richard-Dit-Bressel P, McNally GP (2016): Lateral, not medial, prefrontal cortex contributes to punishment and aversive instrumental learning. Learning & memory. 23:607–617. [PubMed: 27918280]
56. Bossert JM, Stern AL, Theberge FR, Cifani C, Koya E, Hope BT, et al. (2011): Ventral medial prefrontal cortex neuronal ensembles mediate context-induced relapse to heroin. Nature neuroscience. 14:420–422. [PubMed: 21336273]
57. Koya E, Uejima JL, Wihbey KA, Bossert JM, Hope BT, Shaham Y (2009): Role of ventral medial prefrontal cortex in incubation of cocaine craving. Neuropharmacology. 56 Suppl 1: 177–185. [PubMed: 18565549]
58. Warren BL, Mendoza MP, Cruz FC, Leao RM, Caprioli D, Rubio FJ, et al. (2016): Distinct Fos-Expressing Neuronal Ensembles in the Ventromedial Prefrontal Cortex Mediate Food Reward and Extinction Memories. The Journal of neuroscience : the official journal of the Society for Neuroscience. 36:6691–6703. [PubMed: 27335401]
59. Rogers JL, Ghee S, See RE (2008): The neural circuitry underlying reinstatement of heroin-seeking behavior in an animal model of relapse. Neuroscience. 151: 579–588. [PubMed: 18061358]
60. Otis JM, Namboodiri VM, Matan AM, Voets ES, Mohorn EP, Kosyk O, et al. (2017): Prefrontal cortex output circuits guide reward seeking through divergent cue encoding. Nature. 543:103–107. [PubMed: 28225752]
61. Halladay LR, Blair HT (2017): Prefrontal infralimbic cortex mediates competition between excitation and inhibition of body movements during pavlovian fear conditioning. Journal of neuroscience research. 95:853–862. [PubMed: 26997207]
62. Halladay LR, Blair HT (2015): Distinct ensembles of medial prefrontal cortex neurons are activated by threatening stimuli that elicit excitation vs. inhibition of movement. Journal of neurophysiology. 114:793–807. [PubMed: 25972588]
63. Diehl MM, Bravo-Rivera C, Rodriguez-Romaguera J, Pagan-Rivera PA, Burgos-Robles A, Roman-Ortiz C, et al. (2018): Active avoidance requires inhibitory signaling in the rodent prelimbic prefrontal cortex. eLife. 7.
64. Resstel LB, Souza RF, Guimaraes FS (2008): Anxiolytic-like effects induced by medial prefrontal cortex inhibition in rats submitted to the Vogel conflict test. Physiology & behavior. 93:200–205. [PubMed: 17884112]
65. Chen BT, Yau HJ, Hatch C, Kusumoto-Yoshida I, Cho SL, Hopf FW, et al. (2013): Rescuing cocaine-induced prefrontal cortex hypoactivity prevents compulsive cocaine seeking. Nature. 496:359–362. [PubMed: 23552889]
66. Limpens JH, Damsteegt R, Broekhoven MH, Voorn P, Vanderschuren LJ (2015): Pharmacological inactivation of the prelimbic cortex emulates compulsive reward seeking in rats. Brain research. 1628:210–218. [PubMed: 25451128]
67. Ma YY, Lee BR, Wang X, Guo C, Liu L, Cui R, et al. (2014): Bidirectional modulation of incubation of cocaine craving by silent synapse-based remodeling of prefrontal cortex to accumbens projections. Neuron. 83:1453–1467. [PubMed: 25199705]
68. Pascoli V, Terrier J, Espallergues J, Valjent E, O'Connor EC, Luscher C (2014): Contrasting forms of cocaine-evoked plasticity control components of relapse. Nature. 509:459–464. [PubMed: 24848058]
69. Bossert JM, Stern AL, Theberge FR, Marchant NJ, Wang HL, Morales M, et al. (2012): Role of projections from ventral medial prefrontal cortex to nucleus accumbens shell in context-induced reinstatement of heroin seeking. The Journal of neuroscience : the official journal of the Society for Neuroscience. 32:4982–4991. [PubMed: 22492053]
70. Lee AT, Vogt D, Rubenstein JL, Sohal VS (2014): A class of GABAergic neurons in the prefrontal cortex sends long-range projections to the nucleus accumbens and elicits acute avoidance behavior. The Journal of neuroscience : the official journal of the Society for Neuroscience. 34:11519–11525. [PubMed: 25164650]
71. Jean-Richard-Dit-Bressel P, McNally GP (2015): The role of the basolateral amygdala in punishment. Learning & memory. 22:128–137. [PubMed: 25593299]

72. Ghazizadeh A, Ambroggi F, Odean N, Fields HL (2012): Prefrontal cortex mediates extinction of responding by two distinct neural mechanisms in accumbens shell. The Journal of neuroscience : the official journal of the Society for Neuroscience. 32:726–737. [PubMed: 22238108]

73. Al-Hasani R, McCall JG, Shin G, Gomez AM, Schmitz GP, Bernardi JM, et al. (2015): Distinct Subpopulations of Nucleus Accumbens Dynorphin Neurons Drive Aversion and Reward. Neuron. 87:1063–1077. [PubMed: 26335648]

74. Gibson GD, Prasad AA, Jean-Richard-Dit-Bressel P, Yau JOY, Millan EZ, Liu Y, et al. (2018): Distinct Accumbens Shell Output Pathways Promote versus Prevent Relapse to Alcohol Seeking. Neuron. 98:512–520 e516. [PubMed: 29656870]

75. Christakou A, Robbins TW, Everitt BJ (2004): Prefrontal cortical-ventral striatal interactions involved in affective modulation of attentional performance: implications for corticostriatal circuit function. The Journal of neuroscience : the official journal of the Society for Neuroscience. 24:773–780. [PubMed: 14749421]

76. Ambroggi F, Ghazizadeh A, Nicola SM, Fields HL (2011): Roles of nucleus accumbens core and shell in incentive-cue responding and behavioral inhibition. The Journal of neuroscience : the official journal of the Society for Neuroscience. 31:6820–6830. [PubMed: 21543612]

77. Taha SA, Fields HL (2006): Inhibitions of nucleus accumbens neurons encode a gating signal for reward-directed behavior. The Journal of neuroscience : the official journal of the Society for Neuroscience. 26:217–222. [PubMed: 16399690]

78. Krause M, German PW, Taha SA, Fields HL (2010): A pause in nucleus accumbens neuron firing is required to initiate and maintain feeding. The Journal of neuroscience : the official journal of the Society for Neuroscience. 30:4746–4756. [PubMed: 20357125]

79. Millan EZ, Kim HA, Janak PH (2017): Optogenetic activation of amygdala projections to nucleus accumbens can arrest conditioned and unconditioned alcohol consummatory behavior. Neuroscience. 360:106–117. [PubMed: 28757250]

80. Lee BR, Ma YY, Huang YH, Wang X, Otaka M, Ishikawa M, et al. (2013): Maturation of silent synapses in amygdala-accumbens projection contributes to incubation of cocaine craving. Nature neuroscience. 16:1644–1651. [PubMed: 24077564]

81. Holmes A, Fitzgerald PJ, Macpherson KP, Debrouse L, Colacicco G, Flynn SM, et al. (2012): Chronic alcohol remodels prefrontal neurons and disrupts NMDAR-mediated fear extinction encoding. Nature neuroscience. 15:1359–1361. [PubMed: 22941108]

82. DePoy L, Daut R, Brigman JL, Macpherson K, Crowley N, Gunduz-Cinar O, et al. (2013): Chronic alcohol produces neuroadaptations to prime dorsal striatal learning. Proceedings of the National Academy of Sciences of the United States of America. 110:14783–14788. [PubMed: 23959891]

83. Zahr NM, Pfefferbaum A, Sullivan EV (2017): Perspectives on fronto-fugal circuitry from human imaging of alcohol use disorders. Neuropharmacology. 122:189–200. [PubMed: 28118989]

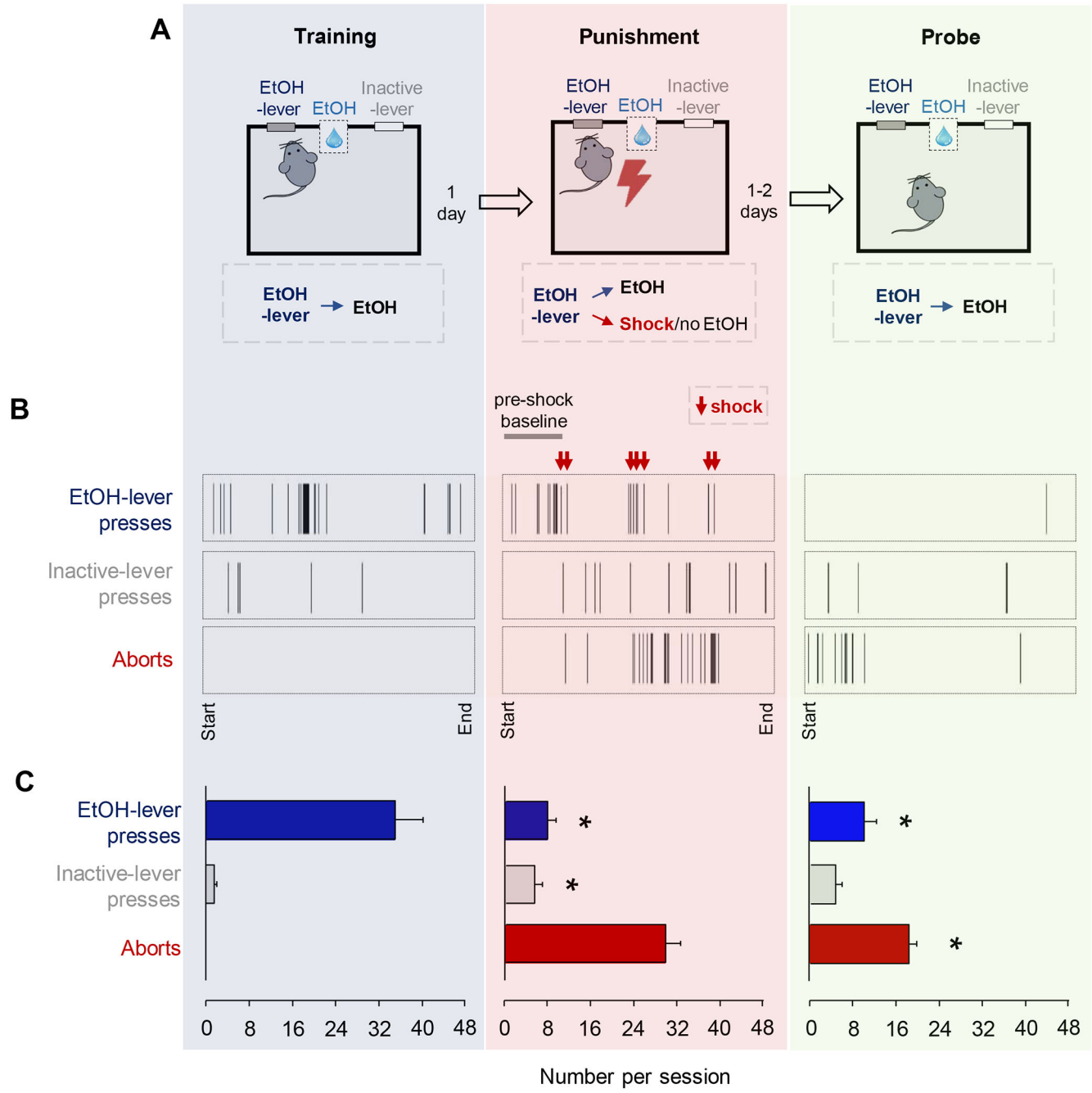

Figure 1: Punished-suppression of EtOH self-administration.

(**A**) Mice were first trained to reliably press 1 of 2 levers for EtOH reward. Following training, there was a punishment session in which, after the first 10 rewarded/unpunished presses (=pre-punishment baseline), presses alternatingly produced either EtOH-reward and no shock, or EtOH-reward and footshock. The day after punishment, there was a probe test in which all presses were rewarded, without shock (i.e., same procedure as during training). (**B**) Example behavioral raster plots showing patterns of EtOH-lever presses, inactive-lever presses and aborts during the last session of training, punishment session (including the pre-

shock baseline period) and probe test. (**C**) The average rate of EtOH-lever presses was significantly lower on the punishment session and probe tests, relative to the pre-punish baseline of the punishment session (repeated measures ANOVA: $F(2,40)=29.00$, $P<0.001$, followed by *post hoc* tests). The rate of inactive-lever presses was slightly but significantly elevated on the punishment session, but not probe tests, relative to pre-punishment baseline (repeated measures ANOVA: $F(2,38)=3.31$, $P=0.047$, followed by *post hoc* tests). Aborts were evident on the punishment session and were maintained, at a significantly lower rate, during the probe tests (paired t-test: $t(19)=4.83$, $P<0.001$). For corresponding head-entry rates, see Figure S1. Data in panel **C** are means ± SEM from n=19-20 mice. *$P<.05$ versus pre-punishment baseline or, in the case of aborts, versus punishment.

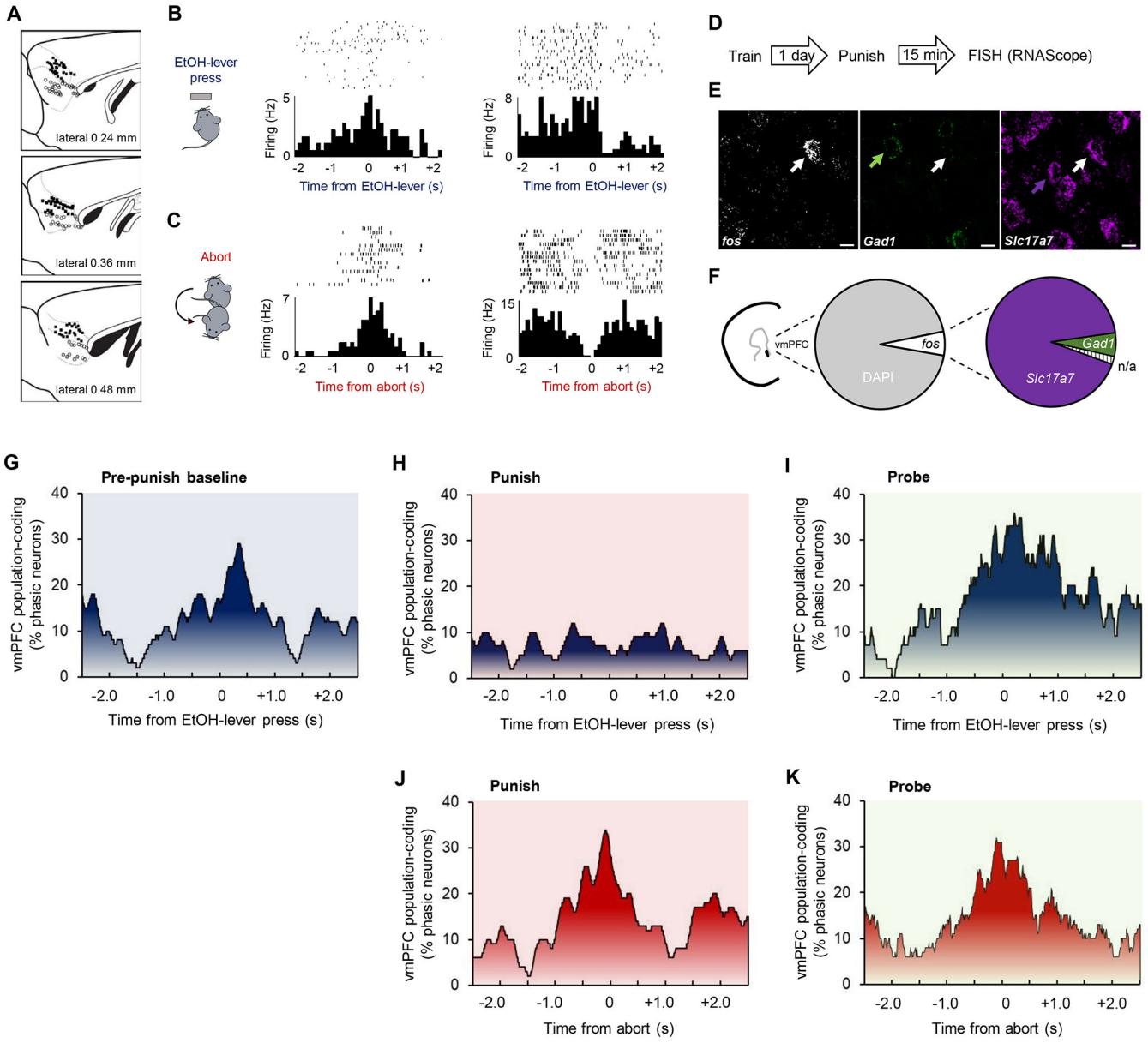

Figure 2: vmPFC encoding of punished-suppression.

(**A**) Location of multi-channel electrode arrays implanted in the vmPFC (open circles) and dmPFC (open circles, for corresponding data, see Figure 4) for *in vivo* neuronal recordings. Example raster plots and peri-event histograms of PFC neurons exhibiting increased or decreased firing as mice made (**B**) EtOH-lever presses and (**C**) aborts. (**D-E**) Following probe testing, vmPFC neurons were labeled for *fos* (c-fos), *Gad1* (Gad67) and *Slc17a7* (vGluT1) mRNA via fluorescence *in situ* hybridization (RNAscope). (**F**) Around 6% of DAPI-labeled neurons in the vmPFC were *fos*-positive after punishment. Of the *fos*-positive cells, the vast majority (91%) were positive for the glutamatergic marker, *Slc17a7,* rather than the GABAergic maker, *Gad1* (7%). Around 2% of *fos*-positive cells were not clearly labeled (n/a) for either marker. (**G**) vmPFC neurons displayed population-level coding for

EtOH-lever presses during the pre-punishment baseline period. (**H**) During the punishment period, there was minimal coding of presses, as a significantly smaller proportion of neurons encoded EtOH-lever pressing during punishment compared to the baseline period (Z=3.36, $P<.001$). (**J**) vmPFC neurons preferentially encoded aborts during the punishment period; a significantly greater proportion of vmPFC neurons encoded abort versus EtOH-lever pressing (Z=4.22, $P<.0001$). There was vmPFC representation of EtOH-lever pressing (**I**) and aborts (**K**) during the probe tests. Data are means ± SEM from a total of n=129 (punished session) and 124 (probe tests) neurons in n=20 mice.

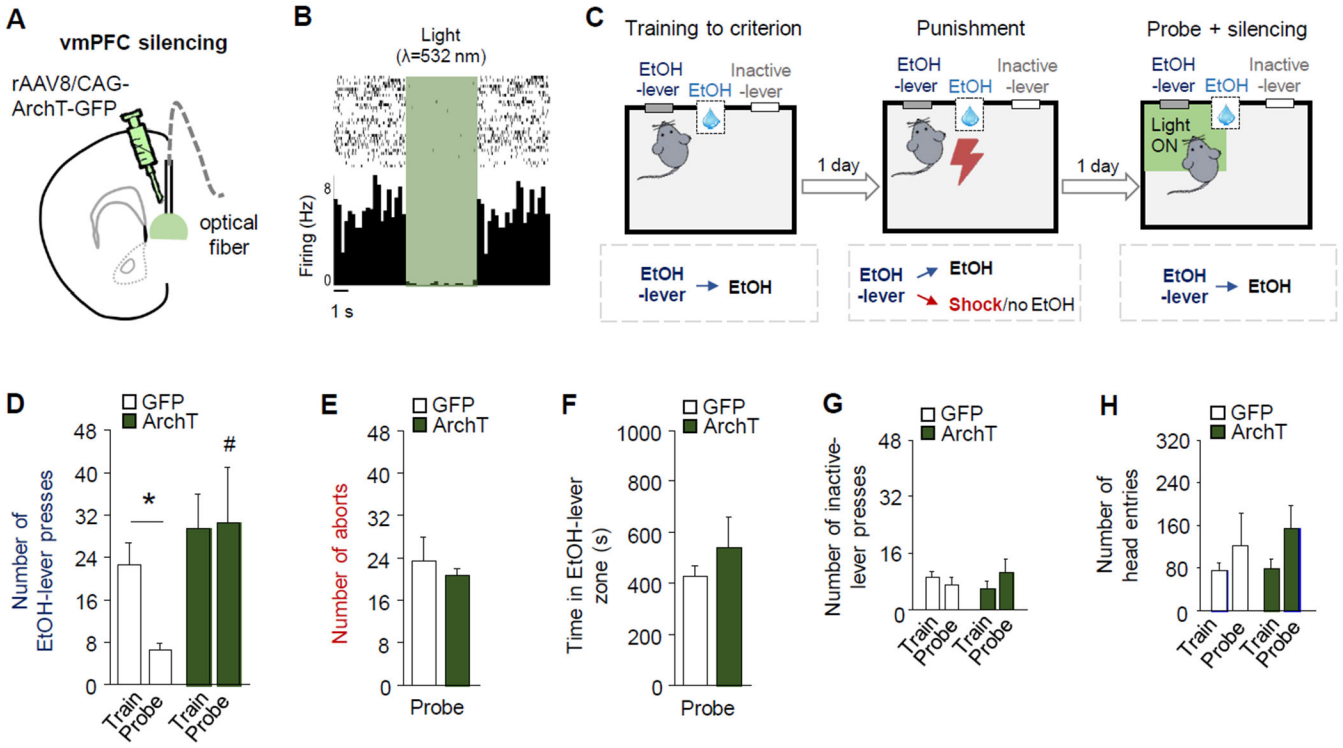

Figure 3: Closed-loop vmPFC-silencing reverses punished-suppression.

(**A**) Optical fibers were bilaterally directed at vmPFC neurons transfected with rAAV8/CAG-ArchT-GFP (ArchT). (**B**) *In vivo* recordings showing vmPFC neuronal inhibition in response to green light. (**C**) Green light was shone to silence vmPFC neurons when mice approached the EtOH-lever during probe testing. (**D**) Difference in EtOH-SA between ArchT and GFP groups (two-way ANOVA, group main effect: F(1,12)=5.91, *P*=. 03). Significant suppression of EtOH-lever pressing during the probe test in GFP controls (mean=22.6 train, 9.3 punishment, 6.6 probe) (paired t-test: t(6)=4.09, P<0.01), but not vmPFC-silenced ArchT group (mean=29.5 train, 7.4 punishment, 30.6 probe) (paired t-test: t(6)=0.08, *P*=0.93), such that the rate on the probe test was significantly higher in the ArchT group than the controls (unpaired t-test: t(12)=2.30, *P*=0.04). GFP and ArchT groups did not differ in (**E**) aborts (unpaired t-test: t(11)=0.52, *P*=0.61) or (**F**) cumulative duration in the light-on zone (unpaired t-test: t(12)=0.88, *P*=0.40). (**G**) The rate of inactive-lever pressing was unaffected by punishment (two-way ANOVA, session main effect: F(1,12)=.001, *P*=.98), but the ArchT group pressed the inactive-lever more than GFP (group main effect: F(1,12)=7.93, *P*=.02). (**H**) The rate of head-entries into the reward-receptacle was unaffected by punishment (two-way ANOVA, session main effect: F(1,12)=2.75, *P*=.12) or group (group main effect: F(1,12)=2.75, *P*=.12). Data are means ± SEM from n=7 mice/group. **P*<.05 versus train in the ArchT group; #*P*<.05 versus probe in GFP controls.

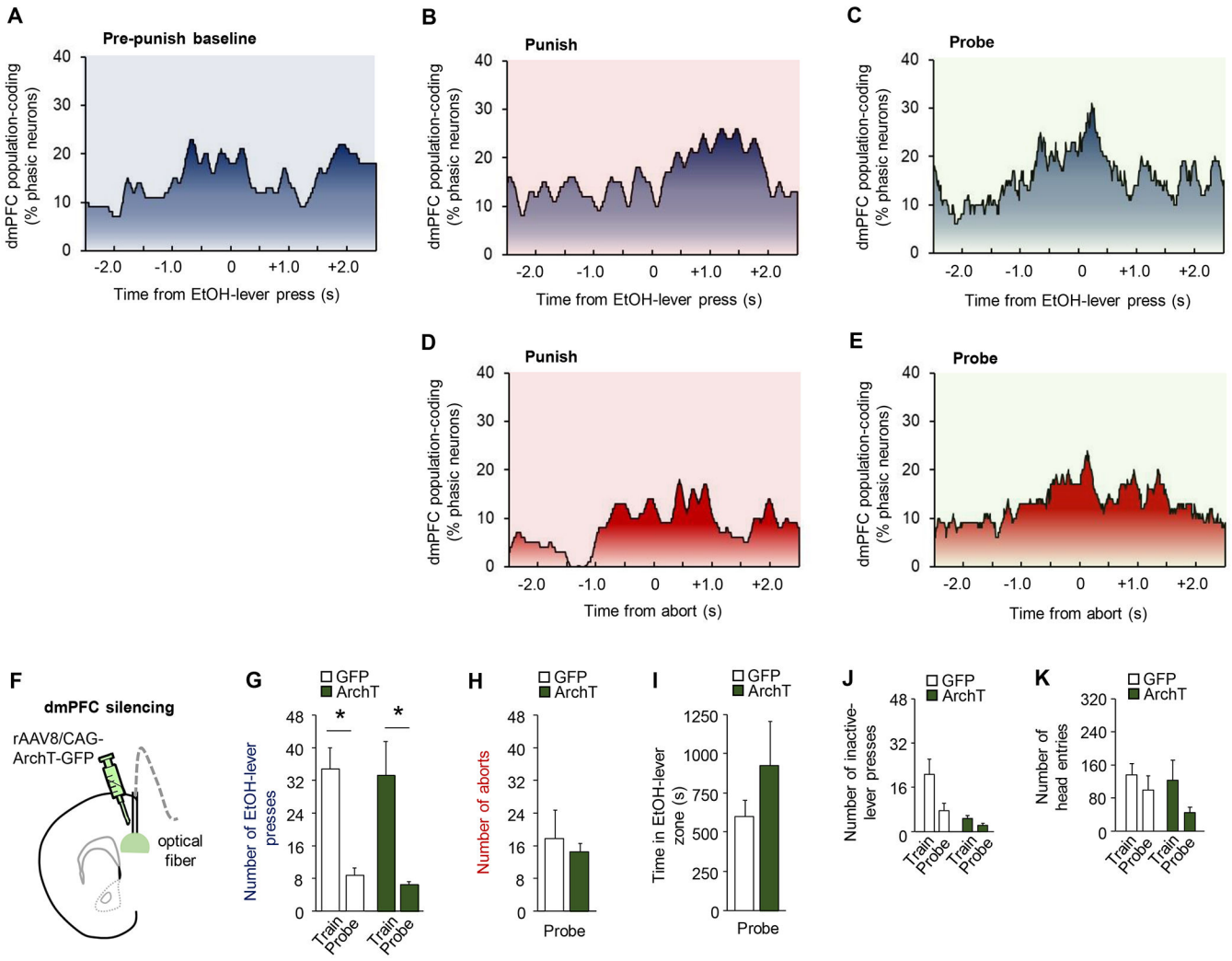

Figure 4. dmPFC encoding of events related to punished-suppression.

dmPFC neurons did not display clear representations of EtOH-lever presses (**A**) during the baseline period before punishment, nor coding of presses (**B**) or aborts (**C**) in the punishment period itself, though there was evidence of some level of press-related coding during the probe trial (**D-E**). (**F**) Optical fibers were bilaterally directed at dmPFC neurons transfected with rAAV8/CAG-ArchT-GFP (ArchT). Green light was shone to silence vmPFC neurons when mice approached the EtOH-lever during probe testing. (**G**) Significant suppression of EtOH-lever pressing during the probe test (two-way ANOVA, session main effect: $F(1,12)=25.50$, $P=.0003$) that did not differ between GFP and ArchT groups (GFP mean= 33.7 train, 8.2 punishment, 9.4 probe; ArchT mean=33.3 train, 6.6 punishment, 6.7 probe) (group main effect: $F(1,12)=.053$, $P=.82$). (**H**) GFP and ArchT groups did not differ in the rate of aborts (unpaired t-test: $t(12)=0.43$, $P=0.67$) or (**I**) time in the light-on zone (unpaired t-test: $t(12)=1.09$, $P=0.30$). (**J**) The rate of inactive-lever presses was higher in GFP versus ArchT groups (two-way ANOVA, group main effect: $F(1,12)=14.37$, $P=.003$) and decreased in all animals following punishment (session main effect: $F(1,12)=5.10$, $P=.04$) (**K**) Rate of head-entries decreased for both groups following punishment (two-way

ANOVA, session main effect: F(1,12)=14.21, *P*=.049), but did not differ between groups (group main effect: F(1,12)=.78, *P*=.39). Data are means ± SEM from a total of n=129 (punished session) and 124 (probe tests) neurons in n=20 mice for **A**-**E**, and n=7 mice/group for **F**-**K**. **P*<.05 versus train in the ArchT group; #*P*<.05 versus probe in GFP controls.

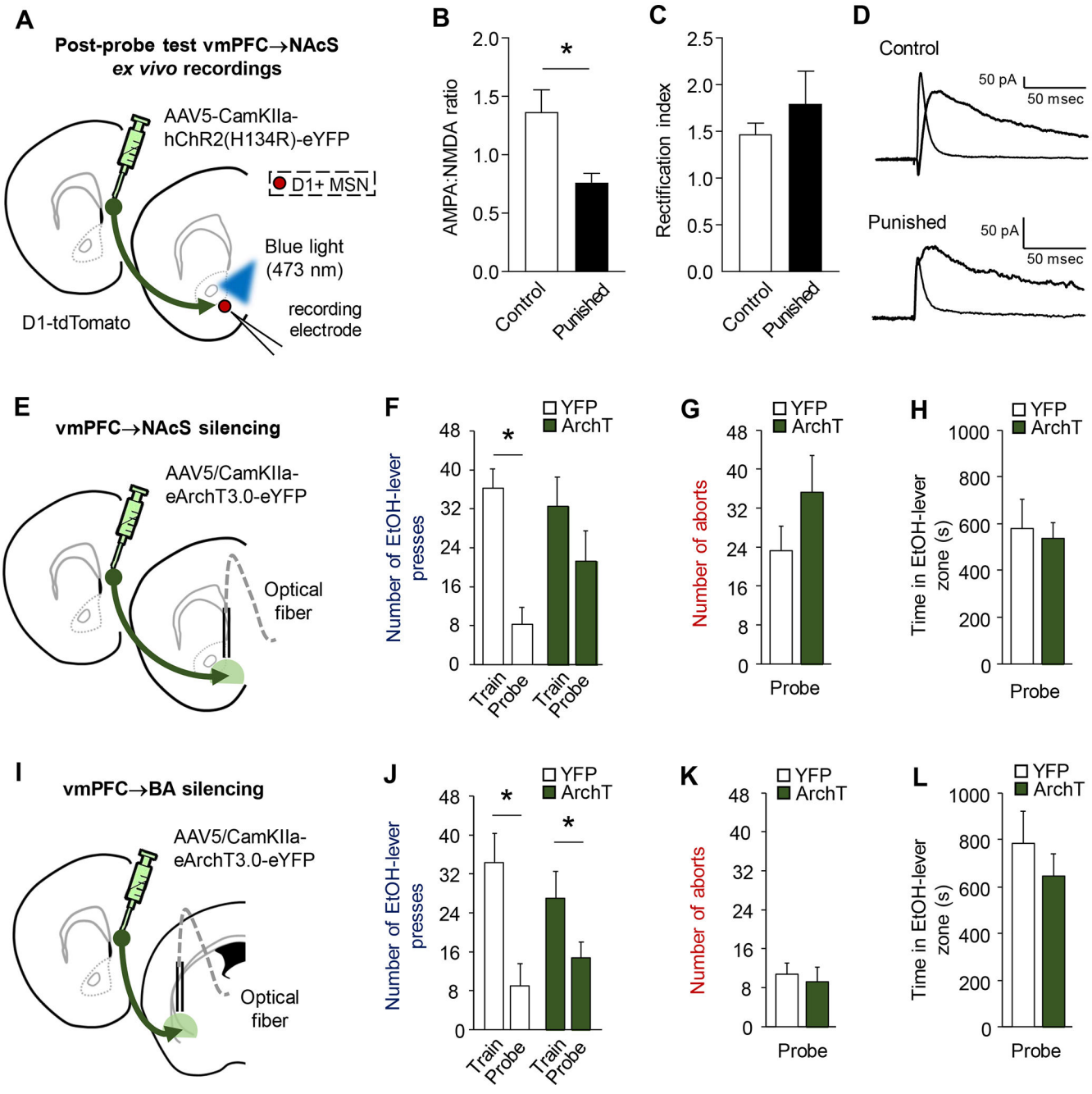

Figure 5: Punishment-related plastic changes in the vmPF→NAcS pathway.

(**A**) Following probe testing, *ex vivo* recordings measured responses of tdTomato-labeled NAcS D1-positive medium spiny neurons to blue light-evoked, ChR2-mediated stimulation of vmPFC inputs. (**B**) There was a significant decrease in AMPA:NMDA ratio in the punished group, as compared to unpunished controls (unpaired t-test: t(17)=2.32, *P*=0.03). (**C**) The rectification index of the AMPA receptor mediated response was not different between groups (unpaired t-test: t(13)=1.09, *P*=0.29). (**D**) Representative traces of AMPA and NMDA synaptic currents evoked by ChR2 stimulation. (**E**) Optical fibers were

bilaterally directed at the NAcS to silence fibers originating from vmPFC neurons transfected with AAV5/CamKII-eArchT3.0-eYFP (ArchT) when mice approached the EtOH-lever during probe testing. (**F**) Punishment reduced EtOH-lever pressing (two-way ANOVA, session main effect: F(1,12)=8.38, *P*=.01). YFP-expressing controls showed a significant decrease in EtOH-lever pressing rate on the probe test, relative to training (mean=36.4 train, 5.5 punishment, 8.3 probe) (paired t-test: t(5)=5.41, P<0.01), whereas the decrease in the ArchT group was modest and non-significant (mean=32.46 train, 8.4 punishment, 21.3 probe) (paired t-test: t(7)= 1.02, *P*=0.34). Further, probe test pressing rates differed significantly between YFP-expressing and ArchT mice (unpaired t-test(12)=1.69, *P*=.034). Neither the rate of (**G**) aborts (unpaired t-test: t(11)=1.07, *P*=0.31) nor the (**H**) time spent in the EtOH-lever zone (unpaired t-test: t(11)=0.54, *P*=0.60) was different between groups. (**I**) Optical fibers were bilaterally directed at the BLA to silence fibers originating from vmPFC neurons transfected with AAV5/CamKII-eArchT3.0-eYFP (ArchT) when mice approached the EtOH-lever during probe testing. (J) The rate of EtOH-lever pressing was significantly lower, as compared to training (two-way ANOVA, session main effect: F(1,10)=17.14, *P*=.002) in both YFP-expressing controls (mean=35.8 train, 12.5 punishment, 7.6 probe) (paired t-test: t(3)=3.31, P<0.05) and the ArchT-expressing group (mean=27.0, 7.6 punishment, 14.7 probe) (paired t-test: t(7)=2.32, *P*=0.05). There were no group differences in the rate of (**K**) aborts (unpaired t-test: t(10)=0.12, *P*=0.91) or (**L**) the time spent in the EtOH-lever zone (unpaired t-test: t(10)=1.33, *P*=0.21). Data are means ± SEM from n=7-12 cells in n=4-9 mice/group in **A-D**, n=6-8 mice/group for **E-H** and n=4-8 mice/group in **I-L**.

KEY RESOURCE TABLE

Resource Type	Specific Reagent or Resource	Source or Reference	Identifiers	Additional Information
Add additional rows as needed for each resource type	Include species and sex when applicable.	Include name of manufacturer, company, repository, individual, or research lab. Include PMID or DOI for references; use "this paper" if new.	Include catalog numbers, stock numbers, database IDs or accession numbers, and/or RRIDs. RRIDs are highly encouraged; search for RRIDs at https://scicrunch.org/resources.	Include any additional information or notes if necessary.
Antibody				
Bacterial or Viral Strain				
Biological Sample				
Cell Line				
Chemical Compound or Drug				
Commercial Assay Or Kit	RNAscope	Advanced Cell Diagnostics	RRID:SCR_012481	
Deposited Data; Public Database				
Genetic Reagent	probes: cfos, vGluT1, gad67, Drd1a, Drd2, Dap	Advanced Cell Diagnostics	c-fos; gene ID 14281, cat#316921, vGluT1; gene ID 72961, cat#416631, Gad67); gene ID 14415, cat#4009	
Organism/Strain	male C57BL/6J; B6.Cg-Tg(Drd1a-tdTomato)6Calak/J m	Jackson Laboratory	RRID:IMSR_JAX:000664; RRID:IMSR_JAX:016204	
Peptide, Recombinant Protein	retrograde tracers Cholera Toxin B-555 and 488	Thermo Fisher Scientific	cat# C34776, 0.5% dilution	
Recombinant DNA				
Sequence-Based Reagent				
Software; Algorithm	CinePlex Behavioral Research Systems; Med-PC softwa	Plexon Inc; Med Associates		
Transfected Construct	AAV5/CaMKIIα-hChR2(H134R)-eYFP; rAAV8/CAG-A	Addgene; UNC Vector Core (Chapel Hill, NC, US	RRID:Addgene_26969	
Other				